Hindawi
International Journal of Distributed Sensor Networks
Volume 2023, Article ID 8931636, 10 pages
https://doi.org/10.1155/2023/8931636

Research Article

Convex Combination for Wireless Localization Using Biased RSS Measurements

Qi Wang[1], **Fei Li**[1], **Teng Shao**[2] and **Chao Xu**[3]

[1]*School of Electronic Engineering, Xi'an Shiyou University, Xi'an, Shaanxi 710065, China*
[2]*School of Electrical and Information Engineering, Anhui University of Science and Technology, Huainan, Anhui 232001, China*
[3]*School of Modern Post, Xi'an University of Posts and Telecommunications, Xi'an, Shaanxi 710061, China*

Correspondence should be addressed to Fei Li; lif@xsyu.edu.cn

Received 17 September 2023; Revised 21 November 2023; Accepted 28 November 2023; Published 20 December 2023

Academic Editor: Antonio Lazaro

Received signal strength- (RSS-) based localization in wireless sensor networks (WSNs) has attracted significant attention due to its advantages of low cost and simple implementation. In practice, RSS measurements may suffer from sensor biases, which deteriorates the localization accuracy. However, most of the existing localization methods are designed for bias-free measurements. In this paper, we propose a convex combination method for RSS localization in the presence of sensor biases. The parameter vector composed of unknown location and sensor biases is estimated simultaneously by using a convex combination of some virtual points. These virtual points form a convex hull, into which the parameter vector falls with large probability. By this, the original nonconvex estimation problem is converted to be convex. Numerical examples demonstrate the superiority of the proposed method in terms of localization accuracy, compared to the existing semidefinite programming (SDP) methods.

1. Introduction

Wireless localization has gained considerable attention in recent years due to its wide applications, such as tracking, mobile communications, and health management [1, 2]. It provides location estimates by using measurements of the physical parameters of a radio signal, including the angle of arrival, time of arrival, time difference of arrival, and RSS [3–5]. Among these, the RSS-based approach has become particularly popular with the advantages of low-cost and easy implementation. For example, a built-in WiFi module in intelligent devices makes RSS measurements easily accessed.

RSS localization is mostly on the basis of the radio propagation path loss model, of which the suitability heavily affects the localization accuracy. In practice, sensor measurements are inevitably subject to a variety of errors, which leads to biased measurement models [6, 7]. The errors involved in the RSS measurements mainly include two types: random error and systematic bias. Systematic bias especially originating from sensors heavily affects localization accuracy, which is usually caused by a design problem or other factors. However, only a few works focus on the RSS localization in the presence of sensor biases.

There have been many RSS-based localization methods in the existing work. The maximum likelihood (ML) method can asymptotically attain the optimality [8]. But the formulated estimation problem is nonconvex, of which the globally optimal solution is difficult to achieve. To overcome this problem, in addition to linear methods [9, 10], optimization-based methods have been extensively studied, such as SDP and second-order cone programming [11–14]. They are all convex so that the globally optimal solution can be guaranteed. Besides, they usually have better accuracy than linear least squares (LS) methods. In addition, range-based localization using RSS or time of arrival measurement has also been studied [15–17]. For example, in [15], a diffusion Gauss-Newton algorithm with cooperation strategy is proposed for solving target localization nonlinear-least-squares problem. However, all RSS localization methods mentioned above are

proposed for bias-free models only. When the RSS measurements reported by sensors contain biases, they will become invalid.

In [18], two localization problems using biased RSS measurements were first studied, i.e., source localization and receiver navigation, and several optimization-based methods were proposed. They transform the biased RSS model and formulate different convex estimation problems using approximation and relaxation. In this paper, for the same localization problems, we propose a totally new method with the scheme of convex combination, which provides better performance than the existing SDP methods [19]. The basic idea is to generate a convex hull, into which the parameter vector composed of unknown location and sensor biases falls with some probability such that the vector can be estimated by a convex combination of some virtual points. To this end, an optimization-based method is proposed to construct the convex hull, of which the vertices are used as the virtual points. Then, the original nonconvex localization problem is converted into a constrained LS problem of calculating combination coefficients. The implementation of the proposed method can be summarized as the following procedures: (1) generating the virtual points; (2) calculating the combination coefficients; and (3) combining the virtual points and coefficients as the final estimate. The novelty of the proposed method is to convert the nonconvex problem of ML estimation to convex problems with respect to the construction of virtual points and the calculation of combination coefficients. Since the formulated problems with respect to the proposed method are all convex, the solution can be easily obtained. Numerical examples demonstrate the performance of the proposed localization method, which shows better localization accuracy than the existing SDP methods.

2. Problem Formulation

Consider a WSN consisting of a single target node and N anchor nodes. Two localization problems are investigated, i.e., source localization and receiver navigation. In source localization, the source node is stationary with unknown location x^o, which acts as a target node and is localized with accumulated measurements of multiple receivers (anchor nodes) of multiple times. The receivers move all the time, and the locations of receiver j are known as $\mathrm{y}_{k,j}$ at time k. In receiver navigation, the receiver moves with unknown locations x_k^o at time k, which acts as a target node and is localized with its received measurements from multiple sources (anchor nodes) at the current time. The sources are stationary, and the location of source j is known as $\mathbf{y}_j$. Accordingly, the RSS measurement model in the presence of sensor biases for the two localization problems can be written as

$$P_{k,j} = P_0 + \Delta_j(\Delta) - 10\beta \log_{10} \frac{d_{k,j}}{d_0} + n_{k,j}, j = 1, \cdots, N, \quad (1)$$

where $P_{k,j}$ is the RSS measurement corresponding to anchor node j at time k, P_0 is the reference power at a reference distance d_0, β is the path loss exponent (P_0 and β are assumed known; $d_0 = 1m$ is usually assumed), $\Delta_j(\Delta)$ is the unknown sensor bias, and $d_{k,j} = \|\mathrm{x}^o - \mathrm{y}_{k,j}\|$ or $d_{k,j} = \|\mathrm{x}_k^o - \mathrm{y}_j\|$ is the distance between the target node and anchor node j at time k. The noise terms $n_{k,j}$ are assumed independent and identically distributed zero-mean Gaussian random variables with variance σ^2 [20]. Note that source localization involves multiple sensor biases while receiver navigation involves single sensor bias, since the measurements in source localization are collected by multiple sensors and the measurements in receiver navigation are collected by a single sensor.

Let θ be the parameter vector to be estimated, which consists of the unknown location and sensor biases. Then, the ML estimators for source localization and receiver navigation can be, respectively, written as

$$\widehat{\theta} = \arg \min_{\theta} \sum_{j=1}^{N} \sum_{s=1}^{k} \left(P_{s,j} - P_0 - \Delta_j + 10\beta \log \frac{d_{s,j}}{d_0} \right)^2, \quad (2)$$

$$\widehat{\theta} = \arg \min_{\theta} \sum_{j=1}^{N} \left(P_{k,j} - P_0 - \Delta + 10\beta \log \frac{d_{k,j}}{d_0} \right)^2. \quad (3)$$

Obviously, both the problems above are nonconvex so that their globally optimal solutions are difficult to achieve. For this, we resort to a convex combination method in this letter. Note that the details of the proposed algorithm will be presented for source localization only since it follows a similar procedure for receiver navigation.

3. Convex Combination Method

3.1. Basic Idea. In source localization, $\theta = [(\mathbf{x}^o)^T, \Delta_1, \cdots, \Delta_N]^T$ is to be estimated. As is well known, any point located inside a convex hull can be represented by a convex combination of the vertices of the hull. According to this, if we have a convex hull such that θ falls inside, θ can be represented by a convex combination of the vertices. That is,

$$\theta = \sum_{i=1}^{m} w_i \mathbf{v}_i, \quad (4)$$

where $\mathbf{v}_i$ is the vertices of the convex hull (also termed as virtual points) with $i = 1, \cdots, m$ and w_i is the convex combination coefficient with $\sum_{i=1}^{m} w_i = 1$ and $w_i \geq 0$.

First, we rewrite the ML estimator of θ in (2) as

$$\widehat{\theta} = \arg \min_{\theta} \sum_{j=1}^{N} \sum_{s=1}^{k} \left\| P_{s,j} - f\left(\theta, \mathbf{y}_{s,j}\right) \right\|^2, \quad (5)$$

where $f(\boldsymbol{\theta}, \mathbf{y}_{s,j}) = P_0 + \boldsymbol{\theta}_{j+3} - 10\beta \log_{10}(d_i(\theta(1:3), \mathbf{y}_{s,j})/d_0)$, $\boldsymbol{\theta}(1:3)$ denotes the unknown source location, and θ_{j+3} denotes the jth sensor's bias.

Input:

The biased RSS measurements, $\mathbf{P} = \{P_{s,j}\}_{s=1,j=1}^{s=k,j=N}$;

The locations of receivers at each time, $\{\mathbf{y}_{s,j}\}_{s=1,j=1}^{s=k,j=N}$;

Output:

An estimate of the source location and sensor biases $\widehat{\theta}$;

1: Generate the virtual points matrix $\mathbf{V}$ by solving the QCQP problem ((13a)–(13d)) with $\mathbf{P}$ and $\{\mathbf{y}_{s,j}\}_{s=1,j=1}^{s=k,j=N}$, and then obtain the matrix $\mathbf{\Phi}$;

2: Obtain the convex combination coefficients $\widehat{\mathbf{w}}$ by solving problem (14) with $\mathbf{P}$ and $\mathbf{\Phi}$;

3: Obtain $\widehat{\theta} = \mathbf{V}\widehat{\mathbf{w}}$;

Algorithm 1: Convex combination method.

Combining (4) with (5), the ML estimator is equal to

$$\widehat{\mathbf{w}} = \arg \min_{\widehat{\mathbf{w}}} \sum_{j=1}^{N} \sum_{s=1}^{k} \left\| P_{s,j} - f\left(\sum_{i=1}^{m} w_i \mathbf{v}_i, \mathbf{y}_{s,j} \right) \right\|^2, \quad (6)$$

with $\mathbf{w} = [w_1, w_2, \cdots, w_m]$.

Next, a mathematical theorem is introduced.

Theorem 1. *Suppose a point set* $\mathbf{V}(\rho) \triangleq \{\mathbf{v}_1(\rho), \mathbf{v}_2(\rho), \cdots, \mathbf{v}_m(\rho)\}$ *form a convex hull,* $\mathbf{v}_i(\rho) \longrightarrow \mathbf{x}$ *when* $\rho \longrightarrow 0$, $i = 1, 2, \cdots, m$. *Let* $r(\rho)$ *be the radius of the bounding ball* $B(\mathbf{V}(\rho))$ *of* $\mathbf{V}(\rho)$, *and* $\mathbf{z}_\infty$ *be a point outside the convex hull. Then, for any finite integer* $m \geq 2$ *and all possible points* $\mathbf{x}$, *we have*

$$\lim_{\rho \longrightarrow 0} \frac{\sum_{i=1}^{m} w_i f(\mathbf{v}_i(\rho), \mathbf{z}_\infty) - f(\sum_{i=1}^{m} w_i \mathbf{v}_i(\rho), \mathbf{z}_\infty)}{r(\rho)} = 0, \quad (7)$$

where $f(\cdot)$ *is the biased RSS measurement function as in (5) and* $\sum_{i=1}^{m} w_i = 1, w_i \in [0, 1]$.

This theorem can be proved by using mathematical induction. The complete proof can be found in the Appendix.

Equation (7) indicates

$$\sum_{i=1}^{m} w_i f(\mathbf{v}_i(\rho), \mathbf{z}_\infty) \approx f\left(\sum_{i=1}^{m} w_i \mathbf{v}_i(\rho), \mathbf{z}_\infty \right) \quad (8)$$

when the convex hull used is sufficiently small.

By applying (8), when a small convex hull is available, problem (6) can be approximated as

$$\widehat{\mathbf{w}} = \arg \min_{\mathbf{w}} \sum_{j=1}^{N} \sum_{s=1}^{k} \left\| P_{s,j} - \sum_{i=1}^{m} w_i f\left(\mathbf{v}_i, \mathbf{y}_{s,j} \right) \right\|^2. \quad (9)$$

3.2. The Generation of Virtual Points. As can be seen from above, the key of the convex combination method is virtual points. We aim to construct a convex region, in which the source falls inside in the sense of probability. Consider model (1), we have the following ring region:

$$r_{s,j} = \left\{ \mathbf{x}^o \left| 10^{\left(\varepsilon_{k,j} - \alpha_{k,j}\sigma\right)/5\beta} \leq \left\| \mathbf{x}^o - \mathbf{y}_{k,j} \right\|^2 \leq 10^{\left(\varepsilon_{k,j} + \alpha_{k,j}\sigma\right)/5\beta} \right. \right\}, \quad (10)$$

where $\varepsilon_{k,j} = P_0 - P_{k,j} + \Delta_j$ and $\alpha_{k,j}$ determines the size of the region, i.e., the probability of the source falling inside. The larger $\alpha_{k,j}$ is, the more likely the source is to fall inside. Obviously, the source is most likely located inside the intersection of all $r_{s,j}$'s with $s = 1, \cdots k$, $j = 1, \cdots, N$, i.e., $\cap_{s=1,j=1}^{s=k,j=N} r_{s,j}$.

By applying the first-order Taylor series expansion for $\alpha_{k,j}$, the ring region (10) can be approximated as

$$r_{k,j}^0 \gamma_j \left(1 - c\alpha_{k,j}\right) \leq \left\| \mathbf{x}^o - \mathbf{y}_{k,j} \right\|^2 \leq r_{k,j}^0 \gamma_j \left(1 + c\alpha_{k,j}\right), \quad (11)$$

where $r_{k,j}^0 = 10^{(P_0 - P_{k,j})/5\beta}$, $\gamma_j = 10^{\Delta_j/5\beta}$, and $c = \ln 10\sigma/5\beta$. That is,

$$r_{k,j}^0 \left(\gamma_j - c\tilde{\alpha}_{k,j}\right) \leq \left\| \mathbf{x}^o - \mathbf{y}_{k,j} \right\|^2 \leq r_{k,j}^0 \left(\gamma_j + c\tilde{\alpha}_{k,j}\right), \quad (12)$$

where $\tilde{\alpha}_{k,j} = \gamma_j \alpha_{k,j}$.

To make the approximation error in (9) small, the region produced by the intersection of all $r_{k,j}$ is supposed to be as

Table 1: Complexity comparison of the methods considered.

Method	Complexity
CCRL	$O\left((k+1)^2(3k+1)N^3\sqrt{2kN+1}\right)$
URSS-SDP	$O\left(((2k+1)(2kN+4))^2N^2\sqrt{2kN+4}\right)$
DRSS-SDP	$O\left(((2k+1)(2kN+4))^2N^2\sqrt{2kN+4}\right)$

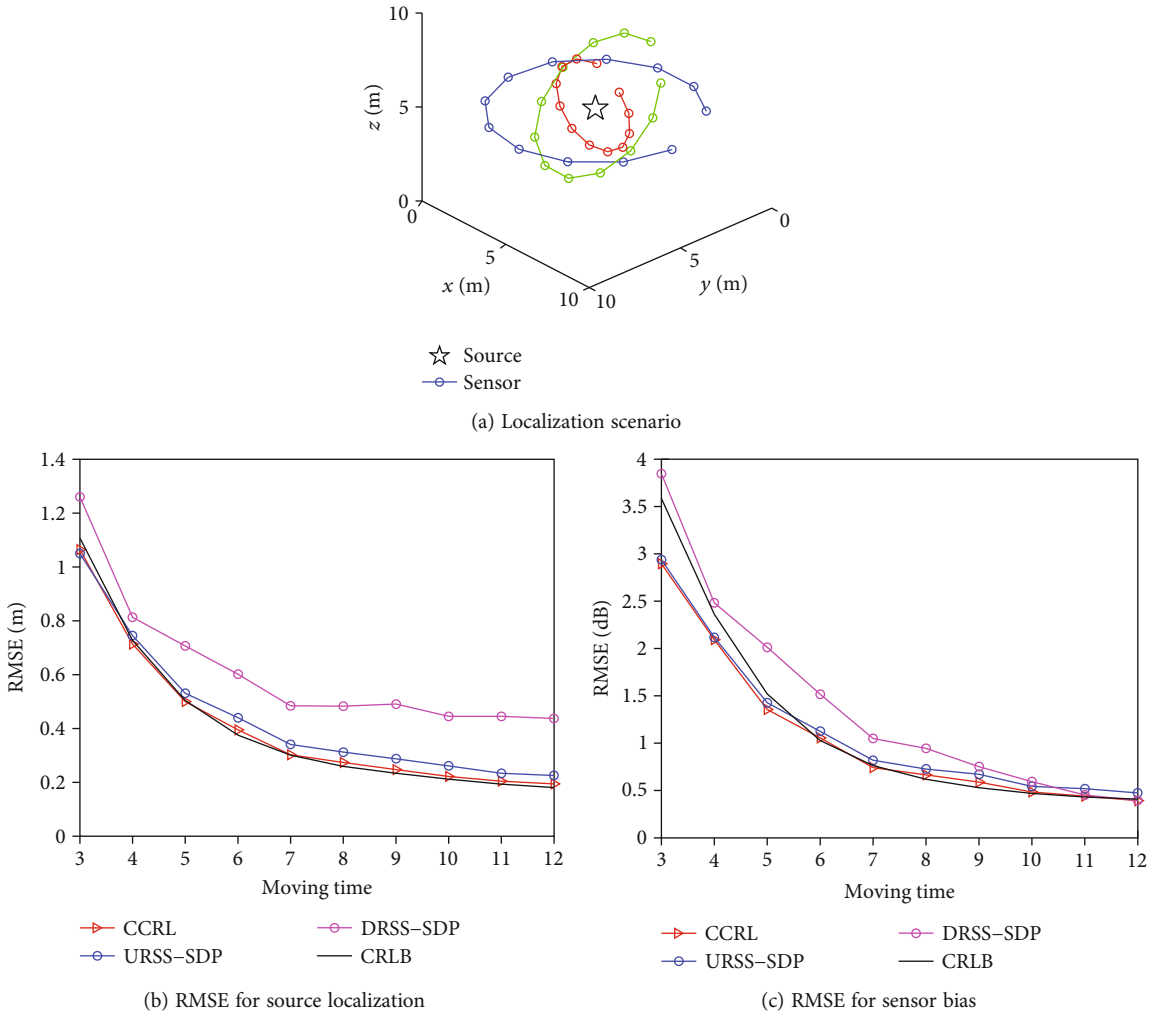

(a) Localization scenario

(b) RMSE for source localization

(c) RMSE for sensor bias

Figure 1: RMSE versus time for source localization.

small as possible. To this end, a quadratically constrained quadratic programming (QCQP) problem is formulated as

$$\arg\min_{x,z,\gamma_j,\tilde{\alpha}_{i,j}} \sum_{j=1}^{N}\sum_{i=1}^{k}\tilde{\alpha}_{i,j}, \tag{13a}$$

$$\text{s.t.} \quad z - 2\mathbf{y}_{i,j}^T\mathbf{x}^o + \mathbf{y}_{i,j}^T\mathbf{y}_{i,j} \geq r_{i,j}^0\gamma_j - cr_{i,j}^0\tilde{\alpha}_{i,j}, \tag{13b}$$

$$z - 2\mathbf{y}_{i,j}^T\mathbf{x}^o + \mathbf{y}_{i,j}^T\mathbf{y}_{i,j} \leq r_{i,j}^0\gamma_j + cr_{i,j}^0\tilde{\alpha}_{i,j}, \tag{13c}$$

$$z \geq (\mathbf{x}^o)^T\mathbf{x}^o. \tag{13d}$$

Remark 2. (1) The objective function (13a) is formulated to make the intersection as small as possible since $\tilde{\alpha}_{i,j}$ determines the width of each ring. (2) The constraints (13b) and (13c) guarantee the existence of the intersection of all ring regions. (3) In (13d), $z = (\mathbf{x}^o)^T\mathbf{x}^o$ is relaxed to $z \geq (\mathbf{x}^o)^T\mathbf{x}^o$ so that it becomes a convex constraint [21].

Denote the solution of θ in problem ((13a)–(13d)) as $\theta^{\mathbf{o}}$. Obviously, it is only a point rather than a convex hull as expected, which can be regarded as a special case of the intersection region. To obtain a convex hull, a multidimensional polyhedron can be expanded with $\theta^{\mathbf{o}}$ being the central point, i.e., $\mathbb{V} = [\theta^{\mathbf{o}}{}_1 + \delta_1, \theta^{\mathbf{o}}{}_1 - \delta_1; \cdots; \theta^{\mathbf{o}}{}_{3+N} + \delta_{3+N}, \theta^{\mathbf{o}}{}_{3+N} - \delta_{3+N}]$, where δ_j indicates the hull size. This is reasonable because θ is intuitively located around the intersection point $\theta^{\mathbf{o}}$ with a large probability. As such, the virtual points $\mathbf{v}_i$ can be generated as the vertices of $\mathbb{V}$. Obviously, there will be 2^{3+N} virtual points.

3.3. Convex Combination Coefficients. With the virtual points, problem (9) is equal to the following constrained LS problem:

$$\widehat{\mathbf{w}} = \arg\min_{\mathbf{w}} \sum_{j=1}^{N}\sum_{s=1}^{k}\left\|P_{s,j} - (\boldsymbol{\Phi}\mathbf{w})_{s\times j}\right\|^2, \tag{14}$$
$$\text{s.t.}\|\mathbf{w}\|_1 = 1, \mathbf{w} \geq \mathbf{0}$$

where $\boldsymbol{\Phi}_{s\times j,i} = f(\mathbf{v}_i, \mathbf{x}_{s,j})$ and $\mathbf{w} = [w_1, \cdots, w_{2^{3+N}}]^T$.

Since the above problem is convex, the combination coefficients can be easily obtained.

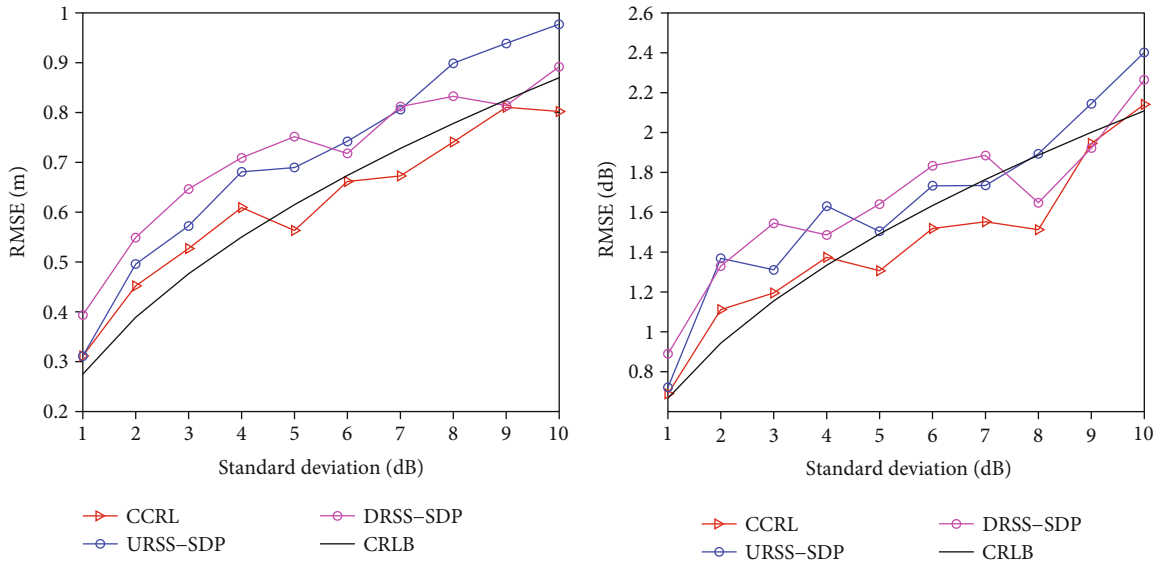

(a) RMSE for source localization

(b) RMSE for sensor bias

Figure 2: RMSE versus noise level for source localization.

3.4. A Summary of the Convex Combination Method. Using the virtual points and combination coefficients obtained in the above subsections, θ can be estimated with the convex combination method. That is, the source location can be estimated by

$$\hat{\mathbf{x}}^o = \mathbf{V}(1:3,:)\hat{\mathbf{w}}, \tag{15}$$

and the sensor bias can be estimated by

$$\hat{\Delta}_j = \mathbf{V}(3+j,:)\hat{\mathbf{w}}, \tag{16}$$

where $\mathbf{V} = [\mathbf{v}_1, \mathbf{v}_2, \cdots, \mathbf{v}_{2^{3+N}}]$. The whole calculation procedures can be summarized as Algorithm 1.

4. Complexity Analysis

In this section, we analyze the computational complexity of the proposed method and compare with the SDP methods in [18]. For the proposed method, it follows the QCQP formulation. Denote the number of variables as m and the number of quadratic constraints as s, respectively, in the following standard QCQP problem.

$$\begin{aligned} &\min && \mathbf{c}^T\mathbf{y} \\ &\text{s.t.} && f_i(\mathbf{y}) = \mathbf{y}^T B_i \mathbf{y} + b_i^T \mathbf{y} + c_i \le 0, i = 1, \cdots, s \end{aligned}, \tag{17}$$

where B_i is an $m \times m$ positive semidefinite symmetric matrix. The arithmetic cost of one step in solving this QCQP problem is dominated by $O((m+s)m^2)$, and the number of iterations is bounded by $O(\sqrt{s})$. Thus, the total complexity is given by $O(s^{0.5}(m+s)m^2)$ [22].

The computational cost of the proposed method mainly includes two parts. One corresponds to obtain an intersection point, and the other corresponds to calculate the convex combination coefficients. Obviously, the two optimization problems in these two parts are both QCQPs. But the latter has a fixed dimension since the number of the virtual nodes is 8. As a result, its cost will be constant and can be neglected when N or k is large enough. That is, the computational complexity of the proposed convex combination RSS localization method (denoted by CCRL) is mainly determined by solving the QCQP problem ((13a)–(13d)). Obviously, for problem ((13a)–(13d)), we have the number of variables $m = k(N+1)+4$ and the number of quadratic constraints $s = 2kN+1$. Then, the computational complexity of the

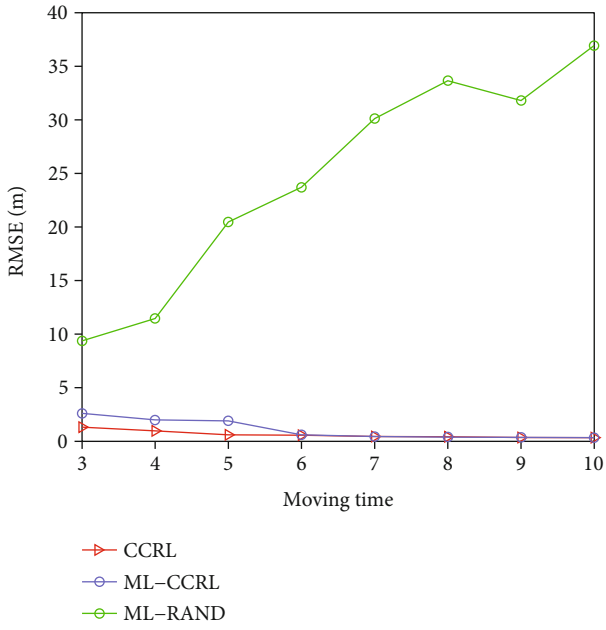

Figure 3: Initialization for ML method.

proposed method can be written as $O((k+1)^2(3k+1)N^3\sqrt{2kN+1})$.

For the SDP methods, their computational complexities can be analyzed by solving a standard SDP problem.

$$\begin{aligned} \min \quad & \mathbf{c}^T\mathbf{y} \\ \text{s.t.} \quad & A(\mathbf{y}) \geq 0 \end{aligned}, \tag{18}$$

where

$$A(\mathrm{y}) = A_0 + \sum_{i=1}^{m} y_i A_i. \tag{19}$$

$\mathbf{y}, \mathbf{c} \in R^m, A_0, \cdots, A_m \in R^{l\times l}$ are symmetric matrices. The computational cost for each iteration is given by $O(m^2l^2)$ at least, where m and l are the numbers of variables and dimensions of the LMI involved, respectively. If the constraints contain k LIMs, we have $l = \sum_{i=1}^{k} l_i$, where l_i is the dimension of the ith LMI. The number of iterations is bounded by $O(\sqrt{l})$. Thus, the total complexity of solving an SDP problem is given by $O(m^2l^{2.5})$.

For both the URSS-SDP and DRSS-SDP methods, we have $m = (2k+1)N + 4$ and $l = 2kN + 4$. Their computational complexities can be written as $O(((2k+1)(2kN+4))^2N^2\sqrt{2kN+4})$ [23, 24].

The computational cost of all methods considered is summarized in Table 1. Obviously, their dominant terms are different. For the proposed CCRL method, it is $O(3k^3N^3\sqrt{2kN+1})$. However, for the URSS-SDP and DRSS-SDP methods, they are both $O(16k^4N^4\sqrt{2kN+4})$. As such, the proposed CCRL method is more computationally efficient than the URSS-SDP and DRSS-SDP methods when the number of sensors N and moving time k are large.

5. Numerical Examples

The performance of the proposed CCRL is demonstrated for both source localization and receiver navigation, in which the RSS measurements suffer from different biases for different sensors. It is also compared with the two SDP methods in [18], i.e., URSS-SDP (URSS-SDP-l_1) and DRSS-SDP (DRSS-SDP-l_1). Besides, the Cramer-Rao lower bound (CRLB) is provided as a benchmark for performance evaluation. The path-loss exponent and reference power were set to $\beta = 3$ and $P_0 = -40$ dB, respectively [25, 26]. The hull size of the proposed method was set to $\delta_n = 0.5$ for all ns, if not specified. All simulation results were averaged over 300 Monte Carlo runs.

5.1. Source Localization. As Figure 1(a) shows, three receivers (sensors) moved around an emission source, of which the true location was $\mathbf{x}^o = [5, 5, 5]^T$, in a 3D circular motion pattern. The true values of sensor biases for the three receivers were $\Delta_1 = 5$ dB, $\Delta_2 = 7$ dB, and $\Delta_3 = 3$ dB, respectively. At each time, the source was localized with the accumulated measurements of all receivers. Figures 1(b) and 1(c) show

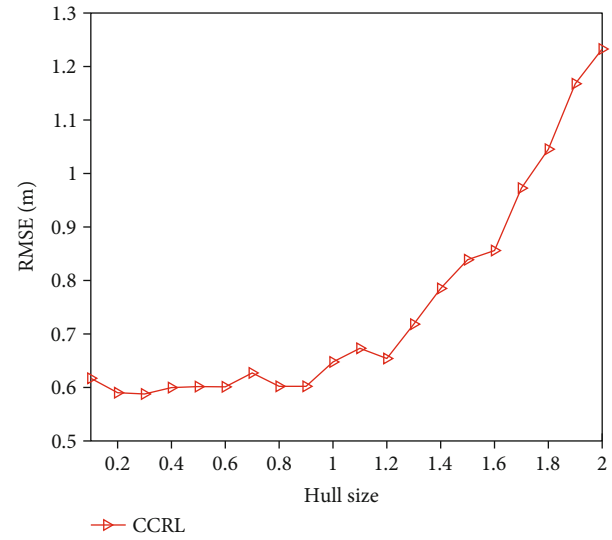

Figure 4: Effect of hull size on RMSE.

the root-mean-square error (RMSE) of each method versus time, where the standard deviation of noise was set to $\sigma = 2$ dB. As is shown, all RMSEs become lower as time goes, since more and more measurements are available. In estimating the source location, the proposed method performs best among all the methods considered, especially much better than the DRSS-SDP method. In estimating sensor bias, taking sensor 3 for instance, the proposed method also shows the superiority in many cases (time 5 to time 9).

Figure 2 shows the RMSE versus noise standard deviation, in which the moving time of receivers was fixed at 7. All RMSEs increase as the noise level grows. Clearly, the proposed method provides the best performance in estimating both location and sensor bias. In some cases, its RMSE is even lower than the CRLB, which is a lower bound for unbiased estimator only [8]. This indicates that the proposed method may be biased.

As mentioned before, the ML method is nonconvex, and its solution heavily depends on the initialization. Figure 3 shows the results of the ML method using different initializations, where ML-RAND and ML-CCRL denote the ML methods initialized with random value and the result of the proposed method, respectively. It can be seen that the ML method performs rather poorly when a random initialization is used. By contrast, the performance is significantly improved when the result of the proposed method is used as the initialization, which verifies the necessity of a good initialization for the ML method. Besides, the CCRL method outperforms the ML-CCRL method at some time (time 3 to 6). This indicates that it is not necessary to refine the ML estimator for better performance in some cases, when an estimation by the proposed method is available.

For the proposed method, the effect of the hull size (δ_j) on the performance has two aspects. On the one hand, a large size helps increase the probability of the target falling inside the convex hull, which contributes to improve localization accuracy. On the other hand, a large size leads to

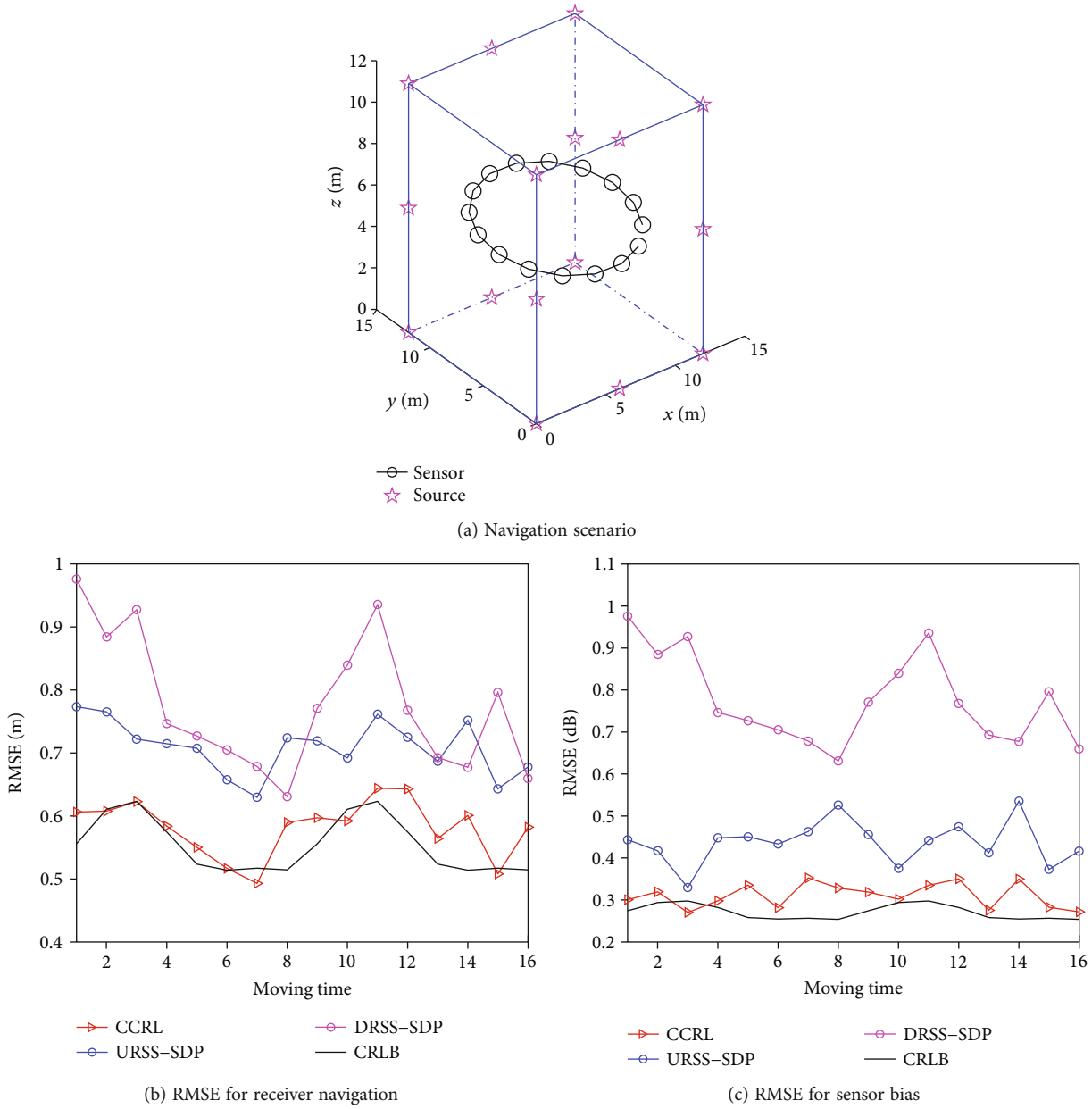

(a) Navigation scenario

(b) RMSE for receiver navigation

(c) RMSE for sensor bias

FIGURE 5: RMSE versus time for receiver navigation.

large approximation error involved in the algorithm, which deteriorates localization accuracy. As Figure 4 shows, the RMSE remains stable when the size is less than 1. This indicates that there is a trade-off between the two aspects. However, when the size gets larger than 1, the RMSE grows quickly. Obviously, in this case, the effect of approximation error involved in the algorithm is dominant. In practice, the selection of δ_j depends on the size of localization scenario. Generally, a larger scenario induces larger errors to the RSS measurements. As a result, a larger δ_j is needed to make the target node fall inside the convex hull with higher probability. As the experiment results show, δ_j can be selected as about 0.5 for a three-dimensional scenario of size $10 \times 10 \times 10$.

5.2. Receiver Navigation. For receiver navigation, we consider the scenario in Figure 5(a), where 16 source nodes were distributed on the boundary of a cube with known coordinates. A receiver (sensor), moved in a circular pattern inside the cube, was localized with the real-time measurements from all source nodes. Figures 5(b) and 5(c) show the RMSEs for navigation and sensor bias versus time, in which the noise standard deviation σ and the true value of sensor bias were set to $\sqrt{2}$ dB and 3 dB, respectively. As is shown, the proposed CCRL method still outperforms both the SDP-URSS and SDP-DRSS methods in all cases. Besides, it is close to the CRLB in some cases.

Figure 6 shows the RMSE versus noise standard deviation for receiver navigation, in which the moving time of

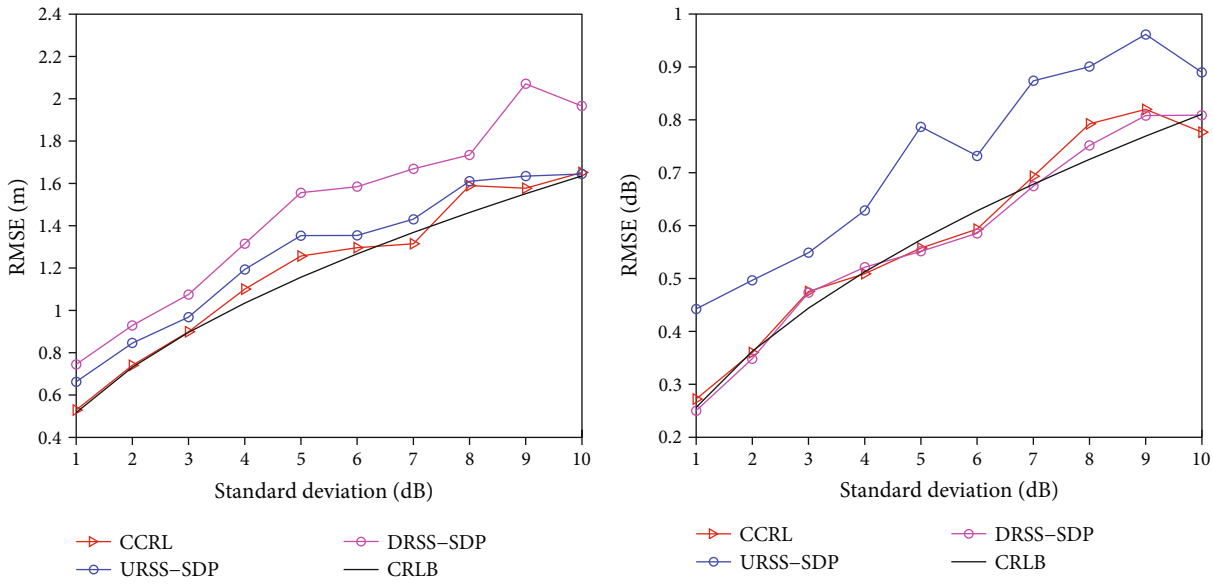

(a) RMSE for receiver navigation

(b) RMSE for sensor bias

Figure 6: RMSE versus noise level for receiver navigation.

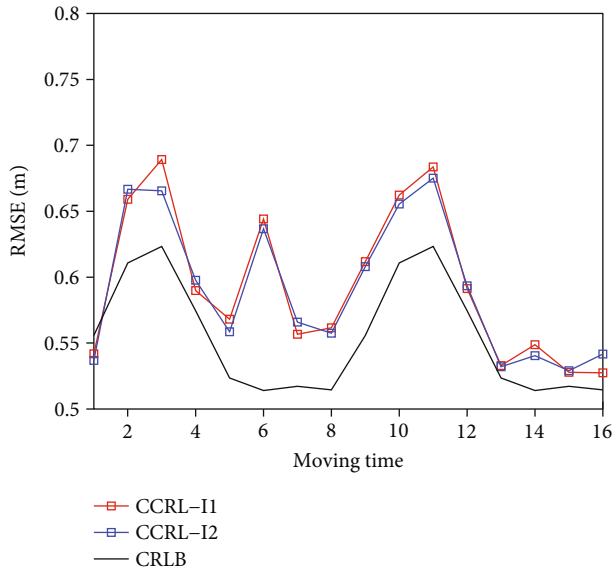

Figure 7: RMSE of receiver navigation with invalid measurements.

the receiver was fixed at 7 and σ still varied from 1 dB to 10 dB. Similar to the results in Figure 2, all RMSEs increase with the growth of noise level. The proposed method performs best in estimating receiver location. As for estimating sensor bias, the proposed method performs close to the DRSS-SDP method and the CRLB. However, the URSS-SDP method does not perform as well as others.

To verify the robustness of the proposed CCRL method, invalid measurements are considered in receiver navigation. Denote the results with 7 and 5 invalid sensor measurements by CCRL-I1 and CCRL-I2, respectively, and each invalid measurement involves with the error of 100 dB. As Figure 7 shows, the CCRL-I1 and CCRL-I2 are still close to the CRLB, which demonstrates the good robustness of the proposed method.

6. Conclusion

In this paper, we propose a convex combination method for RSS-based localization using measurements in the presence of sensor biases. The parameter vector composed of target location and sensor biases is simultaneously estimated by a convex combination of some virtual points. A QCQP problem is formulated to construct the convex hull (virtual points). The combination coefficients are then determined by solving a constrained LS problem. Numerical examples demonstrate the performance of the proposed method. In estimating location, it performs better than the existing URSS-SDP and DRSS-SDP methods for all scenarios considered, and in estimating sensor bias, it also shows superiority in many cases. Besides, it significantly outperforms the ML method with a random initialization.

Appendix

A.1. Proof of Theorem 1

To prove Theorem 1, we use mathematical induction. First, we consider the two-point case (i.e., $m = 2$).

Suppose that the 2D plane is spanned by unit vectors $\mathbf{r}_x$ and $\mathbf{r}_y$. Let $\mathbf{x}$ be at the origin. $\mathbf{v}_1 = -R_1\mathbf{r}_x, \mathbf{v}_2 = R_2\mathbf{r}_x$, R_1 and R_2 are scalars, and $\mathbf{v}_j(\rho) = (1-\rho)\mathbf{x} + \rho\mathbf{v}_j, j = 1, 2$. Thus, $\mathbf{x}$ is in the hull of $\mathbf{V}(\rho)$. The radius of the bounding ball of $\mathbf{V}(\rho)$ is $r(\rho) = \rho(R_1 + R_2)/2$. Let $\mathbf{v}(\rho) = \lambda\mathbf{v}_1(\rho) + (1-\lambda)\mathbf{v}_2(\rho)$. We can see that the hull shrinks to $\mathbf{x}$ as $\rho \longrightarrow 0$. $\mathbf{z}_\infty = h_x\mathbf{r}_x + h_y\mathbf{r}_y = [h_x, h_y]^T$. Let $S_{j,\infty}^{(\rho)} = S(\mathbf{v}_j(\rho), \mathbf{z}_\infty)$, where $S(\cdot)$ is the biased

RSS function. That is,

$$\begin{aligned} S(\mathbf{v}_1(\rho), \mathbf{z}_\infty) &= P_0 + \Delta_{v1}(\rho) - 10\beta \log_{10}\tilde{d}_1, \\ S(\mathbf{v}_2(\rho), \mathbf{z}_\infty) &= P_0 + \Delta_{v2}(\rho) - 10\beta \log_{10}\tilde{d}_2, \\ S(\mathbf{v}(\rho), \mathbf{z}_\infty) &= P_0 + \Delta_{v}(\rho) - 10\beta \log_{10}\tilde{d}_3, \end{aligned} \tag{A.1}$$

where $\mathbf{v}(\rho) = \lambda\mathbf{v}_1(\rho) + (1-\lambda)\mathbf{v}_2(\rho)$, $\Delta_v(\rho) = \lambda\Delta_{v1}(\rho) + (1-\lambda)\Delta_{v2}(\rho)$, $\tilde{d}_1 = \sqrt{h_y^2 + h_z^2 + (h_x + \rho R_1)^2}$, $\tilde{d}_2 = \sqrt{h_y^2 + h_z^2 + (h_x - \rho R_2)^2}$, $\tilde{d}_3 = \sqrt{h_y^2 + h_z^2 + (h_x - \rho R_2 + \lambda\rho(R_1 + R_2))^2}$.

Since $\mathbf{v}_1(\rho)$, $\mathbf{v}_2(\rho)$, and $\mathbf{v}(\rho)$ all shrink to $\mathbf{x}$ as $\rho \longrightarrow 0$,

$$\lim_{\rho\longrightarrow 0} \lambda S(\mathbf{v}_1(\rho), \mathbf{z}_\infty) + (1-\lambda) S(\mathbf{v}_2(\rho), \mathbf{z}_\infty) - S(\mathbf{v}(\rho), \mathbf{z}_\infty) = 0, \tag{A.2}$$

and $\lim_{\rho\longrightarrow 0} r(\rho) = 0$. Then, we have

$$\begin{aligned} &\lim_{\rho\longrightarrow 0} \frac{\lambda S(\mathbf{v}_1(\rho), \mathbf{z}_\infty) + (1-\lambda) S(\mathbf{v}_2(\rho), \mathbf{z}_\infty) - S(\mathbf{v}(\rho), \mathbf{z}_\infty)}{r(\rho)} \\ &= \lim_{\rho\longrightarrow 0} \frac{(\partial/\partial\rho)[\lambda S(\mathbf{v}_1(\rho), \mathbf{z}_\infty) + (1-\lambda) S(\mathbf{v}_2(\rho), \mathbf{z}_\infty) - S(\mathbf{v}(\rho), \mathbf{z}_\infty)]}{\partial(r(\rho))/\partial\rho} \\ &= \lim_{\rho\longrightarrow 0} \frac{\lambda S'(x_1(\rho)) x_1'(\rho) + (1-\lambda) S'(x_2(\rho)) x_2'(\rho) - S'(x_3(\rho)) x_3'(\rho)}{R_1 + R_2/2} \\ &= \lim_{\rho\longrightarrow 0} \frac{-\lambda S'(0) R_1 + (1-\lambda) S'(0) R_2 - S'(0)[-\lambda R_1 + (1-\lambda) R_2]}{R_1 + R_2/2} = 0, \end{aligned} \tag{A.3}$$

where $x_1(\rho)$, $x_2(\rho)$ and $x_3(\rho)$ denote the x coordinates of $\mathbf{v}_1(\rho)$, $\mathbf{v}_2(\rho)$, and $\mathbf{v}(\rho)$, respectively, and the L'Hopital's rule has been used.

Thus, Theorem 1 holds for the two-point case.

Next, we consider the multiple-point case. Suppose that Theorem 1 holds for $m = t \geq 2$, that is,

$$\lim_{\rho\longrightarrow 0} \frac{\sum_{j=1}^{t} \lambda_j S_{j,\infty}^{(\rho)} - S\left(\mathbf{z}_\infty, \sum_{j=1}^{t} \lambda_j \mathbf{v}_j(\rho)\right)}{r(\rho)} = 0. \tag{A.4}$$

For $m = t+1$, we constitute a new point

$$\tilde{\mathbf{v}}_1 = \sum_{j=2}^{t+1} \lambda_j' \mathbf{v}_j(\rho), \tag{A.5}$$

where $\lambda_j' = \lambda_j / 1 - \lambda_1 = \lambda_j / \tilde{\lambda}_1$.

Obviously, $\sum_{j=2}^{t+1} \lambda_j' = (1/1-\lambda_1) \sum_{j=2}^{t+1} \lambda_j = 1$. Thus, we have

$$\lim_{\rho\longrightarrow 0} \frac{\sum_{j=2}^{t+1} \lambda_j' S_{j,\infty}^{(\rho)} - S\left(\mathbf{z}_\infty, \sum_{j=2}^{t+1} \lambda_j' \mathbf{v}_j(\rho)\right)}{r'(\rho)} = 0, \tag{A.6}$$

where $r'(\rho)$ is the radius of $H(\{\mathbf{v}_2(\rho), \cdots, \mathbf{v}_{t+1}(\rho)\})$ (the hull composed by $\mathbf{v}_2(\rho), \mathbf{v}_3(\rho), \cdots, \mathbf{v}_{t+1}(\rho)$).

It can be easily seen that $\mathbf{v}_2(\rho), \mathbf{v}_3(\rho), \cdots, \mathbf{v}_{t+1}(\rho)$ all converge to $\mathbf{x}$ as $\rho \longrightarrow 0$. Thus, $r'(\rho)$ and $r(\rho)$ are infinitesimal of the same order ($\rho \longrightarrow 0$). Then, we have

$$\lim_{\rho\longrightarrow 0} \frac{\sum_{j=2}^{t+1} \lambda_j' S_{j,\infty}^{(\rho)} - S\left(\mathbf{z}_\infty, \sum_{j=2}^{t+1} \lambda_j' \mathbf{v}_j(\rho)\right)}{r(\rho)} = 0. \tag{A.7}$$

That is,

$$\sum_{j=2}^{t+1} \lambda_j' S_{j,\infty}^{(\rho)} = S\left(\mathbf{z}_\infty, \sum_{j=2}^{t+1} \lambda_j' \mathbf{v}_j(\rho)\right) + o[r(\rho)], \tag{A.8}$$

where $o[r(\rho)]$ represents a high-order infinitesimal over $r(\rho)$.

Then, we have

$$\begin{aligned} \sum_{j=1}^{t+1} \lambda_j S_{j,\infty}^{(\rho)} &= \lambda_1 S_{1,\infty}^{(\rho)} + \sum_{j=2}^{t+1} \lambda_j S_{j,\infty}^{(\rho)} = \lambda_1 S_{1,\infty}^{(\rho)} + \sum_{j=2}^{t+1} \tilde{\lambda}_1 \lambda_j' S_{j,\infty}^{(\rho)} \\ &= \lambda_1 S_{1,\infty}^{(\rho)} + \tilde{\lambda}_1 S\left(\mathbf{z}_\infty, \sum_{j=2}^{t+1} \lambda_j' \mathbf{v}_j(\rho)\right) + \tilde{\lambda}_1 o[r(\rho)] \\ &= \lambda_1 S_{1,\infty}^{(\rho)} + \tilde{\lambda}_1 S(\mathbf{z}_\infty, \tilde{\mathbf{v}}_1) + \tilde{\lambda}_1 o[r(\rho)]. \end{aligned} \tag{A.9}$$

From the above, it follows that

$$\begin{aligned} &\lim_{\rho\longrightarrow 0} \frac{\sum_{j=1}^{t+1} \lambda_j S_{j,\infty}^{(\rho)} - S\left(\mathbf{z}_\infty, \sum_{j=1}^{t+1} \lambda_j \mathbf{v}_j(\rho)\right)}{r(\rho)} \\ &= \lim_{\rho\longrightarrow 0} \frac{\lambda_1 S_{1,\infty}^{(\rho)} + \tilde{\lambda}_1 S(\mathbf{z}_\infty, \tilde{\mathbf{v}}_1) + \tilde{\lambda}_1 o[r(\rho)] - S\left(\mathbf{z}_\infty, \lambda_1 \mathbf{v}_1(\rho) + \sum_{j=2}^{t+1} \lambda_j \mathbf{v}_j(\rho)\right)}{r(\rho)} \\ &= \lim_{\rho\longrightarrow 0} \frac{\lambda_1 S_{1,\infty}^{(\rho)} + \tilde{\lambda}_1 S(\mathbf{z}_\infty, \tilde{\mathbf{v}}_1) - S\left(\mathbf{z}_\infty, \lambda_1 \mathbf{v}_1(\rho) + \tilde{\lambda}_1 \sum_{j=2}^{t+1} \lambda_j' \mathbf{v}_j(\rho)\right)}{r(\rho)} + \frac{\tilde{\lambda}_1 o[r(\rho)]}{r(\rho)} \\ &= \lim_{\rho\longrightarrow 0} \frac{\lambda_1 S_{1,\infty}^{(\rho)} + (1-\lambda_1) S(\mathbf{z}_\infty, \tilde{\mathbf{v}}_1) - S(\mathbf{z}_\infty, \lambda_1 \mathbf{v}_1(\rho) + (1-\lambda_1)\tilde{\mathbf{v}}_1)}{r(\rho)} + \frac{\tilde{\lambda}_1 o[r(\rho)]}{r(\rho)} \\ &= \lim_{\rho\longrightarrow 0} \frac{\lambda_1 S(\mathbf{z}_\infty, \mathbf{v}_1(\rho)) + (1-\lambda_1) S(\mathbf{z}_\infty, \tilde{\mathbf{v}}_1) - S(\mathbf{z}_\infty, \lambda_1 \mathbf{v}_1(\rho) + (1-\lambda_1)\tilde{\mathbf{v}}_1)}{r(\rho)} \\ &\quad + \frac{\tilde{\lambda}_1 o[r(\rho)]}{r(\rho)} (\text{two} - \text{point case for } \mathbf{v}_1(\rho) \text{ and } \tilde{\mathbf{v}}_1) = 0. \end{aligned} \tag{A.10}$$

Thus, Theorem 1 holds for all finite numbers m. This completes the proof.

Data Availability

No underlying data was collected or produced in this study.

Conflicts of Interest

The authors declared no potential conflicts of interest with respect to the research, authorship, and/or publication of this article.

Acknowledgments

This research was supported in part by the Natural Science Basic Research Plan in Shaanxi Province of China under Grant No. 2022JQ-641; the Research Program of Young Scholar Innovation Team with the Education Department of Shaanxi Provincial Government under Grant No. 23JP128; the Natural Science Basic Research Program of Shaanxi under Grant No. 2022JQ-726; the National Science Foundation of China under Grant No. U20B2029; the Key Research and Development Program of Shaanxi under Grant No. 2022KW-25; the Shaanxi Qinchuangyuan "Scientist+Engineer" Team Construction Plan under Grant No. 2022kxj-125; and Shaanxi University's Young Scholar Innovation Team and Xi'an Shiyou University's Innovation Team, Natural Science Research Project of Anhui Educational Committee under Grant No. 2023AH051211.

References

[1] N. Saeed, H. Nam, T. Y. Al-Naffouri, and M. Alouini, "A state-of-the-art survey on multidimensional scaling-based localization techniques," *IEEE Communications Surveys and Tutorials*, vol. 21, no. 4, pp. 3565–3583, 2019.

[2] J. Sun, W. Sun, X. Zhang, J. Zheng, C. Tang, and Z. Chen, "Multiuser smartphone-based localization by composite fingerprint descriptors in large indoor environments," *IEEE Sensors Journal*, vol. 23, no. 18, pp. 21882–21893, 2023.

[3] S. Tomic, M. Beko, R. Dinis, and P. Montezuma, "A closed-form solution for RSS/AoA target localization by spherical coordinates conversion," *IEEE Wireless Communications Letters*, vol. 5, no. 6, pp. 680–683, 2016.

[4] J. Zhang and J. Lu, "Analytical evaluation of geometric dilution of precision for three-dimensional angle-of-arrival target localization in wireless sensor networks," *International Journal of Distributed Sensor Networks*, vol. 16, no. 5, Article ID 155014772092047, 2020.

[5] J. Shi, G. Wang, and L. Jin, "Least squared relative error estimator for RSS based localization with unknown transmit power," *IEEE Signal Processing Letters*, vol. 27, pp. 1165–1169, 2020.

[6] X. Li and D. Wang, "A sensor registration method using improved Bayesian regularization algorithm," in *Proceedings of 2nd International Joint Conference on Computational Sciences and Optimization*, pp. 195–199, Sanya, China, 2009.

[7] H. Karniely and H. T. Siegelmann, "Sensor registration using neural networks," *IEEE Transactions on Aerospace and Electronic Systems*, vol. 36, no. 1, pp. 85–101, 2000.

[8] Y. Bar-Shalom, X. R. Li, and T. Kirubarajan, *Estimation with Applications to Tracking and Navigation: Theory Algorithms and Software*, Wiley, New York, 2001.

[9] Y. Xu, J. Zhou, and P. Zhang, "RSS-based source localization when path-loss model parameters are unknown," *IEEE Communications Letters*, vol. 18, no. 6, pp. 1055–1058, 2014.

[10] H. C. So and L. Lin, "Linear least squares approach for accurate received signal strength based source localization," *IEEE Transactions on Signal Processing*, vol. 59, no. 8, pp. 4035–4040, 2011.

[11] H. Lohrasbipeydeh and T. A. Gulliver, "Unknown RSSD-based localization CRLB analysis with semidefinite programming," *IEEE Transactions on Communications*, vol. 67, no. 5, pp. 3791–3805, 2019.

[12] S. Salari, S. Shahbazpanahi, and K. Ozdemir, "Mobility-aided wireless sensor network localization via semidefinite programming," *IEEE Transactions on Wireless Communications*, vol. 12, no. 12, pp. 5966–5978, 2013.

[13] G. Naddafzadeh-Shirazi, M. B. Shenouda, and L. Lampe, "Second order cone programming for sensor network localization with anchor position uncertainty," *IEEE Transactions on Wireless Communications*, vol. 13, no. 2, pp. 749–763, 2014.

[14] H. Lohrasbipeydeh, T. A. Gulliver, and H. Amindavar, "A minimax SDP method for energy based source localization with unknown transmit power," *IEEE Wireless Communications Letters*, vol. 3, no. 4, pp. 433–436, 2014.

[15] M. Wu, N. Xiong, and L. Tan, "Adaptive range-based target localization using diffusion Gauss-Newton method in industrial environments," *IEEE Transactions on Industrial Informatics*, vol. 15, no. 11, pp. 5919–5930, 2019.

[16] X. Fang, C. Wang, T.-M. Nguyen, and L. Xie, "Graph optimization approach to range-based localization," *IEEE Transactions on Systems, Man, and Cybernetics: Systems*, vol. 51, no. 11, pp. 6830–6841, 2021.

[17] F. B. Sorbelli, C. M. Pinotti, S. Silvestri, and S. K. Das, "Measurement errors in range-based localization algorithms for UAVs: analysis and experimentation," *IEEE Transactions on Mobile Computing*, vol. 21, no. 4, pp. 1291–1304, 2022.

[18] Q. Wang, Z. Duan, and X. R. Li, "Three-dimensional location estimation using biased RSS measurements," *IEEE Transactions on Aerospace and Electronic Systems*, vol. 56, no. 6, pp. 4673–4688, 2020.

[19] C. Wang, F. Qi, G. Shi, and X. Wang, "Convex combination based target localization with noisy angle of arrival measurements," *IEEE Wireless Communications Letters*, vol. 3, no. 1, pp. 14–17, 2014.

[20] N. Patwari, A. O. Hero, M. Perkins, N. S. Correal, and R. J. O'Dea, "Relative location estimation in wireless sensor networks," *IEEE Transactions on Signal Processing*, vol. 51, no. 8, pp. 2137–2148, 2003.

[21] S. Boyd and L. Vandenberghe, *Convex Optimization*, Cambridge University Press, Cambridge, UK, 2013.

[22] Y. Nesterov and A. Nemirovskii, *Interior-point polynomial algorithms in convex programming*, SIAM Studies in Applied Mathematics, 2001.

[23] L. Vandenberghe and S. Boyd, "Semidefinite programming," *SIAM Review*, vol. 38, no. 1, pp. 49–95, 1996.

[24] Q. Wang, Z. Duan, and F. Li, "Semidefinite programming for wireless cooperative localization using biased RSS measurements," *IEEE Communications Letters*, vol. 26, no. 6, pp. 1278–1282, 2022.

[25] R. A. Khalil and N. Saeed, "Convex hull optimization for robust localization in ISAC systems," *IEEE Sensors Letters*, vol. 7, no. 12, pp. 1–4, 2023.

[26] T. Rappaport, *Wireless Communications Principles and Practice*, Prentice-Hall, Englewood Cliffs, NJ, USA, 1999.